# Electronic Spectroscopy of Chloro(terpyridine)platinum(II)

**James A. Bailey, Michael G. Hill, Richard E. Marsh, Vincent M. Miskowski, William P. Schaefer, and Harry B. Gray***

Arthur Amos Noyes Laboratory, California Institute of Technology, Pasadena, California 91125

*Received July 1, 1994*[⊗]

The electronic spectrum of $[Pt(tpy)Cl]^+$ (tpy = 2,2′:6′,2″-terpyridine) is influenced dramatically by intermolecular stacking interactions in solution and in the solid state. The crystal structure of $[Pt(tpy)Cl]ClO_4$ (monoclinic, $P2_1/c$ (No. 14); $a = 7.085(2)$, $b = 17.064(5)$, $c = 26.905(8)$ Å; $\beta = 90.0(1)°$; $Z = 8$) consists of discrete $Pt_2$ units (Pt−Pt = 3.269(1) Å) arranged along an infinite tpy-$\pi$ stack (spacing ~ 3.35 Å). Variable-temperature and concentration studies of the absorption and emission spectra of $[Pt(tpy)Cl]^+$ suggest that similar metal−metal and ligand−ligand interactions persist in the solution phase. The high concentration, low-temperature emission spectrum (5:5:1 ethanol:methanol:DMF) reveals a 740-nm band indicative of M−M oligomerization, a 650-nm band attributable to tpy $\pi-\pi$ interactions, and a 470-nm band characteristic of mononuclear $[Pt(tpy)Cl]^+$ $\pi-\pi^*$ emission. Concentration-dependent absorption spectra were fit to a "two-dimer" model, yielding equilibrium constants for the formation of Pt−Pt-, and tpy−tpy-bound dimers of $1.3(1) \times 10^3$ and $1.0(1) \times 10^3$ $M^{-1}$, respectively, in 0.1 M aqueous NaCl. The low temperature solid-state luminescence of $[Pt(tpy)Cl]^+$ is assigned to a $^3$(MMLCT) (MMLCT = metal−metal-to-ligand charge transfer) transition. The energy of this band is highly dependent on the counterion ($PF_6^-$, $ClO_4^-$, $Cl^-$, $CF_3SO_3^-$), in line with the different colors of these various salts. In contrast, the room-temperature solid-state emission spectra are more difficult to interpret. While the red perchlorate salt exhibits a relatively narrow emission band at 725 nm (red-shifted from the 77-K maximum at 695 nm), consistent with a $^3$(MMLCT) transition, the orange ($Cl^-$, $ClO_4^-$, $CF_3SO_3^-$) and yellow ($PF_6^-$) salts have extremely broad room-temperature emission bands that all appear at nearly the same energy ($\lambda_{max}$ ~ 640 nm). We assign this luminescence to an eximeric intraligand transition resulting from $\pi-\pi$ interactions and propose that the temperature dependent emissions from the orange and yellow solid materials originate from multiple electronic states.

## Introduction

Metal−metal bonding between square planar $d^8$ complexes has been extensively investigated in both linear-chain solids (*e.g,* salts of $[Pt(CN)_4]^{2-}$) and in discrete binuclear species (*e.g,* $[Pt_2(\mu\text{-}P_2O_5H_2)_4]^{4-}$).[1,2] In addition, several mononuclear complexes have been shown to oligomerize in solution *via* weak bonding interactions.[3,4] One such complex,[4] $[Pt(tpy)Cl]^+$, precipitates from different solvents (or with different counterions) to give salts of various colors. In our work on the spectroscopy of $[Pt(tpy)Cl]^+$, we have found that both metal-bound $d^8-d^8$ dimers and organic $\pi-\pi$ complexes are present in solution. Since the crystal structure of $[Pt(tpy)Cl]ClO_4$ (recrystallized from DMF/ether) shows both Pt−Pt and tpy−tpy close contacts, it is likely that the different solid-state colors are due to variations in the stacking arrangements of the planar cations.

## Experimental Section

**Instrumentation.** Absorption spectra were measured on either a Cary-14 spectrometer rebuilt by OLIS to include computer control or on a Hewlett-Packard 8452A diode array spectrometer. Corrected emission and emission excitation spectra were measured using the following adaptations from the previously described instrumentation.[5] Light from a Hanovia 200 W Hg/Xe (emission) or 150 W Xe (excitation) lamp mounted in an Oriel 16100 water-cooled lamp housing, equipped with an Oriel 16108 F4.4 ellipsoidal reflector and beam turning assembly, was wavelength selected using a SPEX 1681B 0.22 m Minimate monochromator. The light was then passed through a PAR 125A light chopper (108 Hz) and focused on the sample by a pair of 90° off-axis parabolic mirrors. Emission experiments generally included an appropriate interference filter before the sample. The emitted light was collected at 90° and focused by a second pair of 90° off axis parabolic mirrors. Most experiments utilized an appropriate emission cutoff filter. Data collection and monochromator control were accomplished by computer interface *via* a National Instruments PC-LPM-16 A/D converter to a 386-based PC utilizing in-house software. Both emission and emission-excitation spectra were computer-corrected using files acquired during calibrations. The emission wavelength dependence of a Hamatsu R955 photomultiplier tube was proportioned against the response of a calibrated UV enhanced silicon photodiode to a 150 W Xe lamp. Emission-excitation spectra were proportioned against the 150 W Xe lamp profile obtained from a standard Rhodamine 6G quantum counter. Luminescence decay measurements were made as described previously.[6]

Variable-temperature emission and emission−excitation spectra were measured by immersion of the sample held in a quartz EPR tube into a liquid $N_2$ (77 K) or *n*-pentane/liquid $N_2$ (~150 K) filled quartz-tipped finger dewar. Absorption spectra were measured with the same cooling baths in a dewar fitted with quartz windows. Glassy 77-K solutions were obtained in a 5:5:1 EtOH:MeOH:dimethylformamide (DMF) mixture (abbreviated as EMD), which forms a true, crack-free, transparent glass. Intermediate temperatures were obtained on a sample contained in a sealed quartz tube within a CTI Cryogenics Model 22 refrigerator.

[⊗] Abstract published in *Advance ACS Abstracts,* August 1, 1995.

(1) (a) Miller, J. S., Ed. *Extended Linear Chain Complexes;* Plenum Press: New York, 1982. (b) Keller, H. J., Ed. *Chemistry and Physics of One Dimensional Metals;* Plenum Press: New York, 1977. (c) Gliemann, G.; Yersin, H. *Struct. Bonding* **1985**, *62*, 87. (d) Roundhill, D. M.; Gray, H. B.; Che, C.-M. *Acc. Chem. Res.* **1989**, *22*, 55. (e) Smith, D. C.; Miskowski, V. M.; Mason, W. R.; Gray, H. B. *J. Am. Chem. Soc.* **1990**, *112*, 3759. (f) Marshall, J. L.; Hopkins, M. D.; Miskowski, V. M.; Gray, H. B. *Inorg. Chem.* **1992**, *31*, 5034.

(2) Bailey, J. A.; Miskowski, V. M.; Gray, H. B. *Inorg. Chem.* **1993**, *32*, 369.

(3) (a) Bailey, J. A.; Gray, H. B. *Acta Crystallogr.* **1992**, *C48*, 1420. (b) Bailey, J. A.; Miskowski, V. M.; Gray, H. B. *Acta Crystallogr.* **1993**, *C49*, 793. (c) Yip, H.-K.; Che, C.-M.; Zhow, Z.-Y.; Mak, T. C. *J. Chem. Soc., Chem. Commun.* **1992**, 1369. (d) Ratilla, E. M. A.; Scott, B. K.; Moxness, M. S.; Kostic, N. M. *Inorg. Chem.* **1990**, *29*, 918.

(4) Jennette, K. W.; Gill, J. T.; Sadownick, J. A.; Lippard, S. J. *J. Am. Chem. Soc.* **1976**, *98*, 6159.

(5) Rice, S. F.; Gray, H. B. *J. Am. Chem. Soc.* **1983**, *105*, 4571.

(6) Nocera, D. N.; Winkler, J. R.; Yocom, K. M.; Bordignon, E.; Gray, H. B. *J. Am. Chem. Soc.* **1984**, *106*, 5145.

0020-1669/95/1334-4591$09.00/0 

**Table 1.** Crystal Parameters at 296 K for $[Pt(tpy)Cl]ClO_4$

| | |
|---|---|
| chemical formula | $C_{15}H_{11}N_3Cl_2O_4Pt$ |
| fw | 563.27 |
| space group (No.) | $P2_1/c$ (14) |
| temp, °C | 23 |
| $a$, Å | 7.085(2) |
| $b$, Å | 17.064(5) |
| $c$, Å | 26.905(8) |
| $\beta$, (deg) | 90.0(1) |
| Z | 8 |
| $V$, Å$^3$ | 3252.8(17) |
| $\varrho_{calcd}$, g cm$^{-3}$ | 2.30 |
| $\lambda$, Å | 0.710 73 |
| $\mu$, cm$^{-1}$ | 90.74 |
| transm coeff | 0.785−1.252 |
| $R(F_o^2 > 0)^a$ | 0.039 on $F$ for 1611 reflections |
| $R(F_o^2 > 3\sigma(F_o^2))^a$ | 0.031 on $F$ for 1464 reflections |
| $R_w{}^a$ | 0.005 on $F2$ for 1721 reflections |

$^a$ $R = \sum||F_o| - |F_c||/\sum F_o$; $R_w = \sum w(F_o^2 - F_c^2)^2/\sum w(F_o^2)^2$.

Diffuse reflectance spectra were measured on a modified Cary-17 spectrometer in the laboratory of G. R. Rossman at Caltech.

**Synthesis.** The compound $[Pt(tpy)Cl]Cl\cdot 2H_2O$ was prepared according to the method of Morgan and Burstall[7] as modified by Howe-Grant and Lippard.[8] Counterion metathesis was accomplished by dissolving the chloride salt in water and then precipitating by addition of a large excess of the appropriate salt ($NaClO_4$, $NH_4PF_6$, or $NaCF_3SO_3$). The compounds were recrystallized from DMF ($ClO_4^-$ and $PF_6^-$ salts) or $CH_3CN$ ($CF_3SO_3^-$ salt) by slow diffusion of diethyl ether. The $PF_6^-$ salts of $[Pt(tpy)NH_3]^{2+}$ and $[Pt(tpy)(py)]^{2+}$ (py = pyridine) were prepared by the method reported[9] for the $BPh_4^-$ salt of $[Pt(tpy)(py)]^{2+}$.

**Crystal Structure Determination.** The compound $[Pt(tpy)Cl]ClO_4$ was crystallized as small orange-red blocks by slow diffusion of diethyl ether into a DMF solution that had been recovered from a failed preparation of a phosphine adduct. The crystal used for the diffraction study was an irregular block with dimensions 0.15 × 0.19 × 0.23 mm. Cell dimensions and diffraction intensities were measured on an Enraf/Nonius CAD4 diffractometer with monochromatized Mo Kα radiation using $\omega$ scans: 25 reflections with $6 < \theta < 12°$ were used for cell dimensions. Other crystallographic data are given in Table 1. A hemisphere of data ($\pm h$, $\pm k$, $+l$) was collected out to $2\theta = 40°$ (7269 reflections). These data clearly showed orthorhombic symmetry: the unit-cell angles were at 90° within their esd's and the goodness of fit for averaging the intensities according to *mmm* symmetry was 1.76. However, the systematic absences (*h*0*l*, with *l* odd; 0*k*0 with *k* odd) were characteristic only of the monoclinic space group $P2_1/c$, suggesting that the apparent *mmm* symmetry resulted from twinning (although no actual splitting of spots was observable). Thus, we presumed from the outset that the crystals were twinned, with the structure based on the monoclinic space group $P2/c$; however, all calculations were based on intensities averaged according to Laue symmetry *mmm*, resulting in 1721 independent data. The expected density indicated eight molecules in the unit cell or two per asymmetric unit (in $P2_1/c$).

**Solution and Refinement of Structure.** While solving the structure, we first noted that reflections of the types 0*kl* with *l* odd and *hk*0 with $(h + k)$ odd were systematically weak, although by no means absent. Thus, the structure must conform quite closely to the orthorhombic space group *Pccn*. Indeed, the Patterson function was readily interpreted in terms of a set of eight Pt atoms in general positions of *Pccn*. On this basis, a series of structure-factor, Fourier calculations led to a complete model, with all atoms assigned; after some least-squares refinements, $R$ became 0.13. However, the geometry of the tridentate tpy ligand was quite unsatisfactory, and the most significant feature of this refinement was a splitting of the perchlorate counterion into two half-populated groups, sharing a pair of O atoms but with the Cl atoms on opposite sides of these O's and each having its own pair of additional, half-occupied O atoms. Placing these three atoms (one Cl and two O's) in ordered sites destroyed the orthorhombic symmetry and resulted in a starting model in space group $P2_1/c$.

Initial refinement in $P2_1/c$ was *via* successive structure factor, Fourier cycles, with values of $F^2_{o,hkl}$ and $F^2_{o,\bar{h}kl}$ prorated according to the corresponding $F_c^2$ values. At the beginning, the two values were quite similar, since only three atoms (Cl and two O's) created any difference. As the refinement progressed, the differences grew larger and departure from *Pccn* became more apparent. An encouraging sign was that, as the Pt atoms shifted from *Pccn* symmetry, the ligand geometries improved. This refinement procedure proceeded very slowly (and, indeed, may be effectively singular) because of the large correlations between the model and the proration factors—one for each reflection.

Accordingly, for the final refinements, our full-matrix least-squares program[10] was modified so as to minimize the quantity $\sum w(F_o^2 - (F^2_{c,hkl} + F^2_{c,\bar{h}kl}))^2$. This refinement proceeded routinely to convergence. The hydrogen atoms on the tpy ligand were positioned by calculation (C−H, 0.95 Å) with $B = 1.15B$ of the attached C atom. For the final difference map, we again resorted to the procedure of prorating the $F_o^2$ values according to $F_c^2$.

We made no attempt to refine a twinning ratio; the apparent *mmm* Laue symmetry clearly indicates that the two twin components are very nearly equal, and this was assumed to be so in our refinement. We were unable to determine a precise value for the cell angle $\beta$. The enlarged width of some of the reflections suggests that the angle differs slightly from 90°, but not enough to result in a splitting of the reflections. Accordingly, we estimate that $\beta$ lies within 0.1° of 90°.

## Results

**Structure of $[Pt(tpy)Cl]ClO_4$.** The positional and thermal parameters as well as the calculated distances and angles of $[Pt(tpy)Cl]ClO_4$ are given in Tables 2 and 3.

Figure 1 shows the two independent cations contained in the asymmetric unit. The internal geometries of both cations are very similar to those of many related α-diimine and tris-chelate complexes: a relatively short bond exists between Pt and the central tpy nitrogen (Pt1−N2, 1.952(15) Å; Pt2−N5, 1.933(15) Å; the remaining Pt−N distances are near 2 Å, Table 3), and the restricted bite angle of the tpy ligand results in N−Pt−N angles that are below 90° (N1−Pt1−N2, 81.9(6)°; N2−Pt1−N3, 81.7(7)°; N4−Pt2−N5, 79.8(6)°; N5−Pt2−N6, 81.4(6)°).

As shown in Figure S-1, the cations form a continuous stack along the $x$ direction, with alternating short/long Pt1−Pt2 distances (3.269(1) and 4.197(1) Å, respectively). The short $Pt_2$ dimer unit (Figure 2A) is arranged so that the Pt1−Pt2 vector is nearly perpendicular to the two square planes, with the closest tpy−tpy contacts about 3.35 Å (C1−C26, 3.34(3) Å; C5−N4, 3.35(3) Å). These two cations are rotated with respect to one another at a Cl1−Pt1−Pt2−Cl2 torsional angle of 160°, placing the Cl atoms in a staggered orientation between two rings of the neighboring tpy ligand. The longer Pt−Pt distance (Figure 2B) is caused by a lateral shift of one $[Pt(tpy)Cl]^+$ unit, such that the tpy−tpy contacts across this long Pt−Pt interaction are essentially the same as for the short Pt−Pt distance (C1−C28, 3.36(3) Å; C5−C26′, 3.40(3) Å). The above zigzag arrangement results in a Pt1−Pt2−Pt1′ angle of 143°.

The structure of the perchlorate salt can then be described as either discrete Pt−Pt dimers or as a continuous tpy−tpy-stacked chain.[11] (The upper distance limit for $\pi-\pi$ interactions in organic species is about 3.8 Å;[12] the tpy−tpy separations fall well within this distance for $[Pt(tpy)Cl]ClO_4$ and related complexes.)[4,13] This stacking structure is very similar to that of $[Pt(phbpy)CH_3CN]PF_6$ (Hphbpy = 6-phenyl-2,2′-bipyri-

(7) Morgan, G. T.; Burstall, F. H. *J. Chem. Soc.* **1934**, 1498.
(8) Howe-Grant, M.; Lippard, S. J. *Inorg. Synth.* **1980**, *20*, 101.
(9) Basolo, F.; Gray, H. B.; Pearson, R. G. *J. Am. Chem. Soc.* **1960**, *82*, 4200.
(10) Duchamp, D. J. American Crystallographic Association Meeting, Bozeman, MT; Paper B14, p 29.

**Table 2.** Positional and Temperature Parameters for [Pt(tpy)Cl]$ClO_4$ ($x$, $y$, $z$, and $U_{eq}$[a] × $10^4$ Å$^2$)

| atom | $x$ | $y$ | $z$ | $U_{eq}$ or $B$[a] |
|---|---|---|---|---|
| Pt1 | 377(2) | 2193(0.4) | 582(0.3) | 305(3) |
| Pt2 | 4687(2) | 2864(0.4) | 665(0.3) | 321(3) |
| Cl1 | 1290(11) | 949(3) | 353(3) | 578(19) |
| Cl2 | 3800(10) | 3972(3) | 236(3) | 565(20) |
| Cl3 | 10998(13) | 5821(4) | −3167(3) | 723(24) |
| Cl4 | 4553(12) | 1337(4) | 3315(3) | 690(22) |
| O1 | 9839(46) | 5738(13) | −3582(8) | 1469(95) |
| O2 | 11662(32) | 6603(9) | −3108(7) | 875(64) |
| O3 | 10093(31) | 5550(9) | −2724(6) | 1005(62) |
| O4 | 12597(33) | 5328(10) | −3257(9) | 1270(87) |
| O5 | 4874(33) | 1063(11) | 3800(6) | 1085(80) |
| O6 | 6236(37) | 1299(13) | 3042(9) | 1188(88) |
| O7 | 3890(35) | 2140(10) | 3308(8) | 1262(79) |
| O8 | 3194(34) | 879(12) | 3083(9) | 1271(80) |
| N1 | 496(26) | 2059(9) | 1311(6) | 3.3(4)* |
| C1 | 996(29) | 1412(12) | 1574(8) | 3.1(5)* |
| C2 | 1002(33) | 1407(12) | 2103(9) | 4.2(6)* |
| C3 | 457(43) | 2048(12) | 2346(8) | 4.0(5)* |
| C4 | −30(32) | 2718(11) | 2090(8) | 3.8(5)* |
| C5 | −43(31) | 2728(10) | 1579(7) | 2.5(4)* |
| N2 | −552(24) | 3227(8) | 772(6) | 2.5(3)* |
| C6 | −564(30) | 3375(11) | 1249(7) | 2.8(4)* |
| C7 | −1200(32) | 4145(12) | 1408(8) | 3.5(5)* |
| C8 | −1679(36) | 4664(13) | 1042(10) | 4.4(6)* |
| C9 | −1618(30) | 4476(11) | 551(9) | 3.9(5)* |
| C10 | −929(31) | 3717(11) | 409(8) | 3.1(5)* |
| N3 | 23(31) | 2639(9) | −100(6) | 3.8(4)* |
| C11 | −714(32) | 3405(12) | −77(8) | 3.5(5)* |
| C12 | −1142(35) | 3782(12) | −526(10) | 4.3(6)* |
| C13 | −829(35) | 3462(14) | −953(9) | 5.0(6)* |
| C14 | −70(41) | 2711(14) | −982(9) | 5.8(6)* |
| C15 | 295(30) | 2314(11) | −537(8) | 3.8(5)* |
| N4 | 4433(25) | 3274(8) | 1371(6) | 2.6(3)* |
| C21 | 3929(32) | 4025(13) | 1512(9) | 4.3(6)* |
| C22 | 3885(32) | 4203(12) | 2002(9) | 4.4(5)* |
| C23 | 4374(38) | 3698(13) | 2353(9) | 5.4(6)* |
| C24 | 4945(45) | 2947(12) | 2216(8) | 4.8(6)* |
| C25 | 4902(30) | 2768(11) | 1717(7) | 3.2(4)* |
| N5 | 5466(24) | 1948(8) | 1034(5) | 2.3(3)* |
| C26 | 5513(32) | 1977(11) | 1528(7) | 2.9(5)* |
| C27 | 6080(30) | 1324(11) | 1808(9) | 4.1(5)* |
| C28 | 6616(38) | 655(13) | 1537(9) | 4.8(6)* |
| C29 | 6648(34) | 630(13) | 1024(9) | 3.8(5)* |
| C30 | 6025(26) | 1335(10) | 770(7) | 2.1(4)* |
| N6 | 5284(28) | 2155(8) | 85(6) | 2.9(3)* |
| C31 | 5968(27) | 1439(10) | 235(7) | 1.8(4)* |
| C32 | 6457(32) | 890(12) | −124(9) | 3.9(5)* |
| C33 | 6322(38) | 1038(13) | −620(10) | 5.5(6)* |
| C34 | 5522(36) | 1772(12) | −759(9) | 4.9(5)* |
| C35 | 5111(30) | 2314(10) | −383(8) | 3.0(5)* |

[a] $U_{eq} = {}^1/_3\sum_i\sum_j[U_{ij}(a^*_i a^*_j)(\vec{a}_i\cdot\vec{a}_j)]$. An asterisk denotes the isotropic temperature parameter, $B$.

dine),[14] which shows aromatic ring separations that are much more evenly spaced (3.3, 3.7 Å) than the alternating Pt−Pt separations (3.28(1), 4.59(1) Å). Stacks have been observed in the crystal structures of many aromatic organic compounds,[12] and we have reported[15] a diphenyltriazenido−Pt(tpy) complex that crystallizes with stacks of $\pi-\pi$ interactions between tpy and the phenyl rings of the terminal ligand (closest $\pi-\pi$ contacts of 3.2−3.4 Å) and no short Pt−Pt interactions (shortest Pt−Pt distance equal to 6.91 Å).

**Table 3.** Selected Distances and Angles for [Pt(tpy)Cl]$ClO_4$[a]

| | Distance/Å | | |
|---|---|---|---|
| Pt1−Pt2 | 3.269(1) | N4−C25 | 1.31(3) |
| Pt1−Cl1 | 2.302(7) | C21−C22 | 1.35(3) |
| Pt1−N1 | 1.976(16) | C22−C23 | 1.33(3) |
| Pt1−N2 | 1.952(15) | C23−C24 | 1.39(4) |
| Pt1−N3 | 2.003(18) | C24−C25 | 1.38(3) |
| Pt2−Cl2 | 2.301(6) | C25−C26 | 1.51(3) |
| Pt2−N4 | 2.033(15) | N5−C26 | 1.33(3) |
| Pt2−N5 | 1.933(15) | N5−C30 | 1.32(2) |
| Pt2−N6 | 2.018(6) | C26−C27 | 1.40(3) |
| C27−C28 | 1.41(3) | C28−C29 | 1.38(3) |
| C29−C30 | 1.45(3) | C30−C31 | 1.45(3) |
| N6−C31 | 1.37(3) | N6−C35 | 1.29(3) |
| C31−C32 | 1.39(3) | C32−C33 | 1.36(3) |
| N1−C1 | 1.36(3) | C33−C34 | 1.43(3) |
| N1−C5 | 1.40(3) | C34−C35 | 1.40(3) |
| C1−C2 | 1.42(3) | N2−C6 | 1.31(3) |
| C2−C3 | 1.33(3) | N2−C10 | 1.31(3) |
| C3−C4 | 1.38(3) | C6−C7 | 1.45(3) |
| C4−C5 | 1.38(3) | C7−C8 | 1.37(3) |
| C5−C6 | 1.46(3) | C8−C9 | 1.36(3) |
| C9−C10 | 1.44(3) | C11−C12 | 1.40(3) |
| C10−C11 | 1.42(3) | C12−C13 | 1.29(3) |
| N3−C11 | 1.41(3) | C13−C14 | 1.39(4) |
| N3−C15 | 1.31(30 | C14−C15 | 1.40(3) |
| N4−C21 | 1.38(3) | | |
| | Angle/deg | | |
| Cl1−Pt1−N2 | 176.6(5) | Cl1−Pt1−N1 | 98.4(5) |
| N1−Pt1−N2 | 81.9(6) | Cl1−Pt1−N3 | 98.1(5) |
| N2−Pt1−N3 | 81.7(7) | N1−Pt1−N3 | 163.5(7) |
| Pt1−N1−C5 | 113.8(12) | Pt1−N1−C1 | 128.6(14) |
| Pt1−N2−C10 | 116.6(13) | Pt1−N2−C6 | 115.8(13) |
| Pt1−N3−C15 | 129.9(15) | Pt1−N3−C11 | 111.0(13) |
| Cl2−Pt2−N5 | 178.8(5) | Cl2−Pt2−N4 | 99.3(5) |
| N4−Pt2−N5 | 79.8(6) | Cl2−Pt2−N6 | 99.4(5) |
| N5−Pt2−N6 | 81.4(6) | N4−Pt2−N6 | 161.2(6) |
| Pt2−N4−C25 | 114.4(13) | Pt2−N4−C21 | 126.8(13) |
| Pt2−N5−C30 | 116.7(12) | Pt2−N5−C26 | 119.3(13) |
| Pt2−N6−C35 | 127.3(14) | Pt2−N6−C31 | 112.4(12) |
| C2−C1−N1 | 121.9(19) | C5−N1−C1 | 117.6(16) |
| C4−C3−C2 | 120.5(22) | C3−C2−C1 | 119.1(21) |
| C4−C5−N1 | 120.1(17) | C5−C4−C3 | 120.8(20) |
| C6−C5−C4 | 128.1(18) | C6−C5−N1 | 111.8(16) |
| N2−C6−C5 | 116.5(17) | C10−N2−C6 | 127.3(17) |
| C7−C6−N2 | 117.7(18) | C7−C6−C5 | 125.6(18) |
| C9−C8−C7 | 122.6(22) | C8−C7−C6 | 116.8(20) |
| C11−C10−C9 | 128.3(19) | C10−C9−C8 | 118.8(20) |
| C15−N3−C11 | 119.1(18) | C9−C10−N2 | 116.4(18) |
| N3−C11−C10 | 115.4(18) | C11−C10−N2 | 115.2(18) |
| C14−C13−C12 | 120.4(23) | C12−C11−C10 | 126.8(20) |
| C15−C14−C13 | 117.9(22) | C12−C11−N3 | 117.8(19) |
| C14−C15−N3 | 122.3(20) | C13−C12−C11 | 122.4(22) |
| C24−C23−C22 | 118.9(23) | C25−N4−C21 | 118.7(17) |
| C25−C24−C23 | 117.3(22) | C22−C21−N4 | 118.8(20) |
| C24−C25−N4 | 123.3(19) | C23−C22−C21 | 122.8(22) |
| N5−C26−C25 | 111.3(17) | C26−C25−N4 | 115.1(17) |
| C27−C26−C25 | 127.8(18) | C26−C25−C24 | 121.5(19) |
| C27−C26−N5 | 120.9(18) | C30−N5−C26 | 123.9(16) |
| C29−C30−N5 | 119.4(17) | C28−C27−C26 | 116.3(20) |
| C31−C30−N5 | 115.3(16) | C29−C28−C27 | 123.2(22) |
| C31−C30−C29 | 125.3(17) | C30−C29−C28 | 116.2(20) |
| C32−C31−N6 | 119.0(18) | C35−N6−C31 | 120.3(17) |
| C33−C32−C31 | 122.6(21) | N6−C31−C30 | 114.1(16) |
| C34−C33−C32 | 116.7(22) | C32−C31−C30 | 126.8(18) |
| C34−C35−N6 | 123.0(19) | C35−C34−C33 | 118.1(21) |

[a] Estimated standard deviations are given in parentheses.

(11) For comparison, [Pt(tpy)Cl]$CF_3SO_3$ packs in a closely related stacked structure (Yip, H.-K.; Cheng, L.-K.; Cheung, K.-K.; Che, C.-M. *J. Chem. Soc., Dalton Trans.* **1993**, 2933.) with alternating $Pt_2$ distances (3.328(1) and 3.575(1) Å). However, the "long" Pt−Pt distance of the triflate salt is significantly shorter than the long Pt−Pt distance of the perchlorate salt, and is almost aligned with the short Pt−Pt vector (Pt−Pt−Pt, 169°). This results in corresponding tpy−tpy contacts of about 3.5 Å (as compared to about 3.3 Å for the interaction corresponding to the short Pt−Pt distance in the perchlorate structure). The triflate structure is more appropriately described as discrete dimers in both Pt−Pt and tpy−tpy interactions.

(12) Hunter, C. A.; Sanders, J. K. M. J. *Am. Chem. Soc.* **1990**, *112*, 5525.

(13) (a) Jennette, K. W.; Lippard, S. J.; Vassiliades, G. A.; Bauer, W. R. *Proc. Natl. Acad. Sci. U.S.A.* **1974**, *71*, 3839. (b) Wong, Y.-S.; Lippard, S. J. *J. Chem. Soc., Chem. Commun.* **1977**, 824. (c) Dewan, J. C.; Lippard, S. J.; Bauer, W. R. *J. Am. Chem. Soc.* **1980**, *102*, 858.

(14) Constable, E. C.; Henney, R. P. G.; Leese, T. A.; Tocher, D. A. *J. Chem. Soc., Chem. Commun.* **1990**, 513.

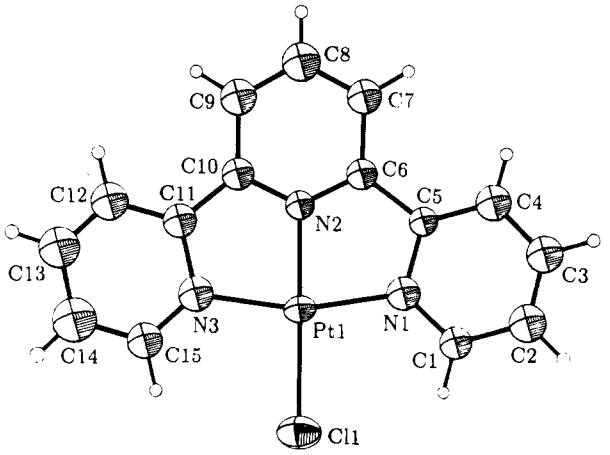


**Figure 1.** ORTEP drawing of one of the two independent cations (showing the numbering scheme) in the structure of $[Pt(tpy)Cl]ClO_4$. The second independent cation is virtually identical with that shown, and has a numbering scheme with the carbon, nitrogen, platinum and chlorine atom numbers incremented by, respectively, 20, 3, 1, and 1. Atoms are shown as 50% probability ellipsoids. Hydrogen atoms are shown as spheres of arbitrary size.

**Solid-State Spectroscopy.** The solid-state properties of $[Pt(tpy)Cl]^+$ salts are highly dependent on the counterion used in precipitation. For example, the perchlorate, chloride, and hexafluorophosphate salts, as precipitated from aqueous solution and vacuum-dried, are deep red, orange, and yellow, respectively. Moreover, recrystallization from other solvents may yield completely different colors; thus, the perchlorate salt recrystallizes from DMF/ether as a rust-orange solid (red-orange when macroscopically crystalline). By analogy to Pt–bpy (bpy = 2,2′-bipyridine)[16] and $[Pt(tpy)]_2(\mu\text{-L})^{3+}$ complexes,[2] it is likely that the range of colors of the $[Pt(tpy)Cl]^+$ salts[17] is due both to the variation of metal–metal separations, and to the degree of oligomerization in the solid state (*via* both metal–metal and $\pi$–$\pi$ interactions).

Solid-state luminescence data for a series of $[Pt(tpy)Cl]^+$ salts are given in Table 4. Given that the crystalline orange perchlorate and triflate[11] salts contain discrete $Pt_2$ units (Pt–Pt distances = 3.269(1) ($ClO_4^-$) and 3.328(1) Å ($CF_3SO_3^-$)), we assign the visible absorptions to a singlet-singlet transition involving $d\sigma^*(Pt_2) \rightarrow \pi^*(tpy)$ (metal–metal-to ligand charge transfer, MMLCT) excited states. Similar assignments have been made for ligand-bridged $[Pt(tpy)]_2(\mu\text{-L})^{3+}$ complexes in solution,[2] and for solid-state linear-chain Pt(II)(α-diimine) compounds.[1abc,16] The low-temperature emissions, which we assign to the corresponding $^3$(MMLCT) states, are narrow (fwhm $\approx$ 1000–2000 $cm^{-1}$) and asymmetric, showing a long tail to lower energy that suggests unresolved vibronic structure in tpy vibrational modes.[16]

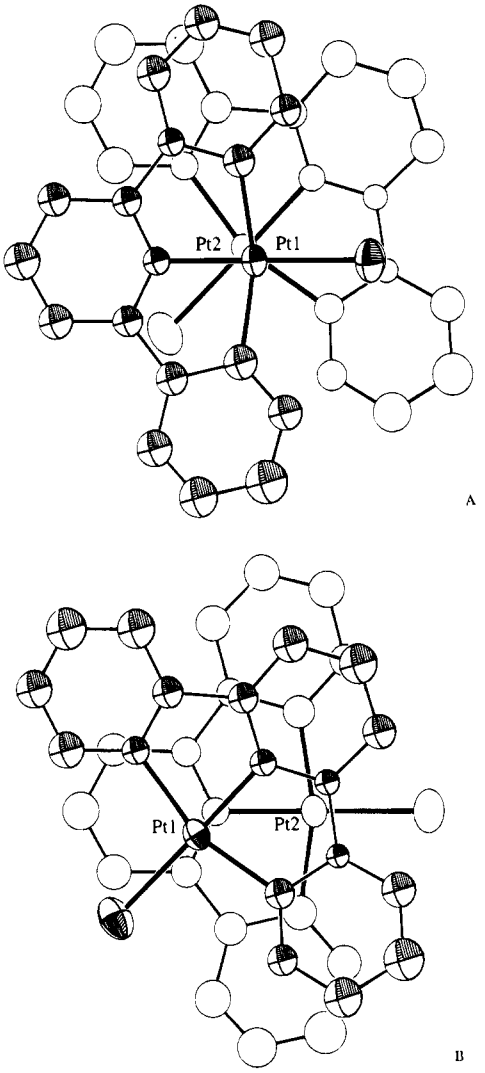


**Figure 2.** ORTEP drawings, showing the two types of cation–cation interactions along the $[Pt(tpy)Cl]^+$ chains of $[Pt(tpy)Cl]ClO_4$, as viewed perpendicular to the average planes of the cations: A, short Pt–Pt distance (3.269(1) Å); B, long Pt–Pt distance (4.197(1) Å). The perpendicular distances between the average planes are nearly identical for interaction A (3.31 Å) and interaction B (3.39 Å). Atoms are shown as 50% probability ellipsoids.

**Table 4.** Emission Maxima for [Pt(tpy)Cl]X Solids

| | $\lambda_{max}$/nm (fwhm/$cm^{-1}$) | |
|---|---|---|
| $X^-$ | 300 K | 77 K |
| $ClO_4^-$ [a] | 725 (2260) | 695 (2010) |
| $ClO_4^-$ [b] | 645 (3100) | 640 (1500) |
| $Cl^-$ [a] | 650 (3350) | 640 (1740) |
| $CF_3SO_3^-$ [c] | 640 (4250) | 625 (1470) |
| $PF_6^-$ [b] | 630 (3850) | 565 (1950) |

[a] Precipitated from aqueous solution and vacuum-dried. [b] Crystallized from DMF/ether. [c] Crystallized from $CH_3CN$/ether.

The absorption and emission properties of the orange chloride salt (from water) are nearly identical with those of the orange perchlorate (from DMF/ether) and triflate salts, so a similar structure is probable. The red perchlorate and yellow hexafluorophosphate salts likely have related structures, but with significantly shorter ($ClO_4^-$) and longer ($PF_6^-$) Pt–Pt distances.

(15) Bailey, J. A.; Catalano, V. J.; Gray, H. B. *Acta Crystallogr.* **1993**, *C49*, 1598.

(16) (a) Houlding, V. H.; Miskowski, V. M. *Coord. Chem. Rev.* **1991**, *111*, 145 and references therein. (b) Miskowski, V. M.; Houlding, V. H.; Che, C.-M.; Wang, Y. *Inorg Chem.* **1993**, *32*, 2518. (c) Miskowski, V. M.; Houlding, V. H. *Inorg. Chem.* **1991**, *30*, 4446. (d) Connick, W. B. Unpublished results.

(17) The reflectance spectra for the salts of $[Pt(tpy)Cl]^+$ are shown in Figure S-2. The onset of the lowest energy intense band is considerably shifted to lower energy ($PF_6^-$ ~570; $ClO_4^-$ (orange), $Cl^-$, ~630; $ClO_4^-$ (red), ~700 nm) with respect to the absorption spectrum measured for a dilute solution, ~420 nm. While the $Cl^-$ salt shows a peak maximum at 517 nm, the remaining compounds exhibit only broad visible absorptions that tail to long wavelength. We have not measured low-temperature reflectance spectra for these materials; however, none appears to change color with temperature.

(18) The temperature independence of this emission maximum contrasts with the room- and low-temperature emission spectra of Pt(α-diimine) complexes having a single Pt–Pt distance that is constant along an infinite linear chain.[16] Thermal lattice contraction necessarily shortens the Pt–Pt distance for this structural type, which accounts quantitatively for the thermal effects.[1c] None of the compounds in this study exhibits this type of behavior; hence none is likely to have a linear chain in the solid state.

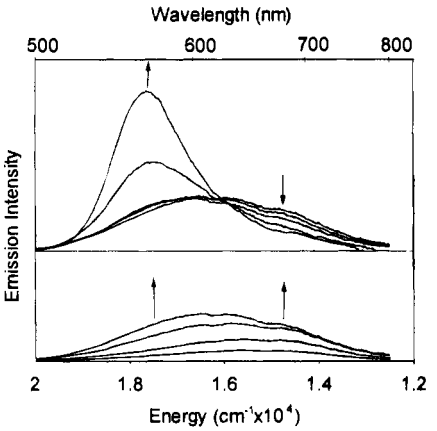


**Figure 3.** Variable-temperature emission spectra for a solid sample of $[Pt(tpy)Cl]PF_6$ (436-nm excitation). Lower set in order of *increasing* intensity at 680 nm: 294, 260, 220, 160 K. Upper set in order of *decreasing* intensity at 680 nm: 160, 140, 120, 100, 70 K.

For the *red* perchlorate salt, the emission band at room temperature is roughly one-third as intense, slightly broadened, and slightly red-shifted relative to the 77-K feature. These luminescence properties are analogous to those of discrete Pt–tpy dimers with short Pt–Pt bonds,[2] in which the emission originates from a $^3$(MMLCT) excited state.[18] In contrast, the room-temperature luminescence spectra of all the other salts show very broad emission bands (fwhm 3000–4250 $cm^{-1}$; maxima in the 630–650-nm region) that are probably not MMLCT in origin. For the orange compounds, the positions of the room-temperature and 77-K maxima are very similar, so the change in bandwidth with temperature can be attributed to thermal broadening (of unknown origin) of a single emission. However, the huge shift (1830 $cm^{-1}$) with temperature for the emission maximum of the yellow $PF_6^-$ salt is very unusual. As shown in Figure 3, from 295 down to about 160 K, the emission exhibits little change in either $\lambda_{max}$ (630 nm) or fwhm, but simply increases in intensity in a regular manner. As the solid is cooled below 160 K, the intensity at 630 nm decreases, while a new narrow band grows in rapidly with $\lambda_{max}$ at 565 nm. By 70 K, the narrow emission is completely dominant, and no further change in the emission profile occurs down to 10 K.[19]

We conclude from the unusual temperature effects that the broad room-temperature and narrow low-temperature emissions for the orange and yellow materials represent two *different* electronic transitions. They may be from two different excited states of the same chromophore, or from two different sites in the solid.[20] In either case, the temperature dependence need not necessarily be Boltzmann-like (as it clearly is not from our observations): the nonradiative rates characteristic of the two emissions may have different temperature dependences, and the state energies themselves may be temperature dependent, owing to lattice contraction.[1c] However, since the thermal transition between the two types of emissions of the $PF_6^-$ salt is not particularly sharp, a simple phase change is probably not involved.

**Solution Luminescence Spectroscopy.** In dilute (< 10 $\mu$M) glassy solution at 77 K, excitation of $[Pt(tpy)Cl]^+$ at 366 nm results in a highly structured luminescence beginning at about 470 nm (vibronic progression ~ 1400 $cm^{-1}$; Franck–Condon simulations give good fits for two modes with frequencies near 1100 and 1450 $cm^{-1}$). This luminescence is virtually identical with that of $[Pt(tpy)(NH_3)]^{2+}$, and is very similar to that

(19) Houlding, V. H. Unpublished results.
(20) Unfortunately, all efforts to prepare X-ray diffraction quality crystals of the $PF_6^-$ salt failed, yielding only fibrous aggregates.

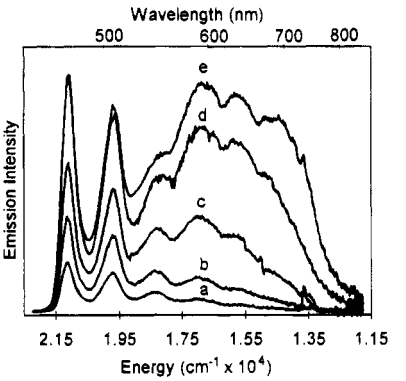


**Figure 4.** Concentration (mM) dependence of the emission spectrum of $[Pt(tpy)Cl]PF_6$ in EMD at 77 K (366-nm excitation): (a) 0.006; (b) 0.0132; (c) 0.03; (d) 0.072; (e) 0.15.

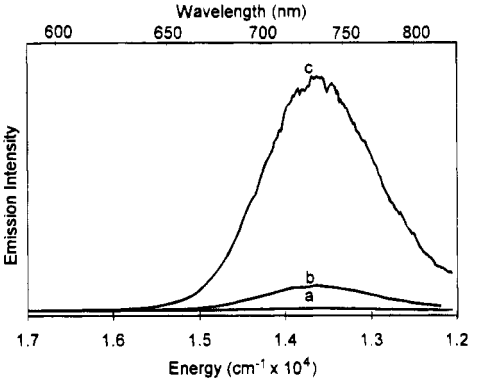


**Figure 5.** Concentration (mM) dependence of the emission spectrum of $[Pt(tpy)Cl]PF_6$ in EMD at 77 K (547-nm excitation): (a) 0.003; (b) 0.072; (c) 0.15.

previously reported[21] for $[Pt(bpy)(en)]^{2+}$ and $[Pt(bpy)_2]^{2+}$ in dilute glasses. A $^3(\pi^* \rightarrow \pi)$ assignment is suggested, with the excitation being largely localized on the α-diimine ligand.[22]

The band shape of the luminescence changes dramatically as the concentration is increased through the range 6 to 150 $\mu$M (Figure 4). Specifically, at least two additional features appear at high concentration: a narrow, unstructured, low-energy band centered at 720 nm, and a broad, weakly structured band at ~ 600 nm.[23] Excitation at 547 nm, *below the onset of the dilute solution emission,* gives only the lowest energy emission band (Figure 5).

Interestingly, a broad, midrange emission also appears for highly concentrated, glassy solutions of free terpyridine. Such concentration-dependent luminescence of aromatic molecules is usually termed "excimeric" emission,[24] although ground-state complexes (probably very weakly bound) are, of course, implicated in emission from rigid glassy matices. Figure 6 shows an overlay of the emission spectra from a high concentration sample of terpyridine (0.1 mM), a low-concentration sample of $[Pt(tpy)Cl]^+$ (0.006 mM), and a combined sample (all in EMD glassy solution at 77 K). At low concentration, the emission spectrum of terpyridine (not shown) is highly structured with

(21) (a) Miskowski, V. M.; Houlding, V. H. *Inorg Chem.* **1989**, *28*, 1529. (b) Maestri, M.; Sandrini, D.; Balzani, V.; von Zelewsky, A.; Deuschel-Cornioley, C.; Jolliet, P. *Helv. Chim. Acta* **1988**, *71*, 1053.
(22) Interestingly, the lowest-energy excited state of $[Pt(bpy)Cl_2]$ is $^3$(d–d).[16b]
(23) This structure may in part be vibronic (there is a poorly-defined spacing of about 1500 $cm^{-1}$), but the complicated behavior as a function of temperature and excitation wavelength suggests that the band may be composite in nature.
(24) (a) Birks, J. B. *Photophysics of Aromatic Molecules;* Wiley-Interscience: New York, 1970. (b) Birks, J. B.; Dyson, D. J.; Munro, I. H.; *Proc. R. Soc. London, A* **1963**, *275*, 575.

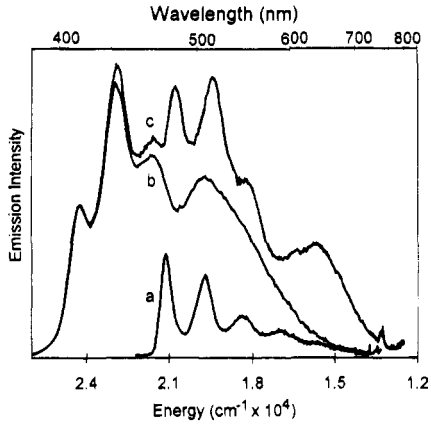


**Figure 6.** Emission spectra (366-nm excitation) in EMD at 77 K of (a) 0.006 mM $[Pt(tpy)Cl]^+$, (b) 0.1 mM tpy, and (c) 0.006 mM $[Pt(tpy)Cl]^+$ and 0.1 mM tpy.

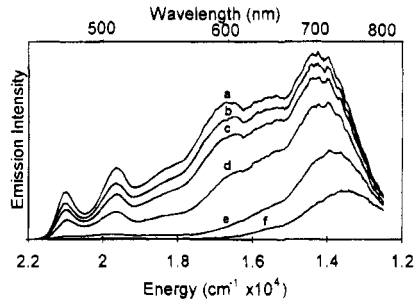


**Figure 7.** Variable temperature (K) emission spectra of 0.18 mM $[Pt(tpy)Cl]PF_6$ in EMD (366-nm excitation): (a) 70; (b) 90; (c) 100; (d) 110; (e) 130; (f) 150.

the same 1400-$cm^{-1}$ progression observed for metal−tpy mononuclear species, but shifted to higher energy. At high concentration (trace b), the profile changes, increasing in intensity and broadening in the middle range of the spectrum. Addition of $[Pt(tpy)Cl]^+$ to this solution (trace c) results in a new emission band at ~625 nm, which must arise from an interaction of terpyridine with the platinum complex.

The temperature dependence of the $[Pt(tpy)Cl]^+$ luminescence is shown in Figure 7. The intensity of the entire spectrum remains virtually constant at temperatures below the glass transition temperature (~115 K), with only a slight decrease as the temperature is increased. As the sample is warmed through the glass transition, the intensity falls off sharply for all but the longest wavelength emission; the latter persists up to about 150 K, above which temperature the intensity decreases beyond detectable limits.

**Emission−Excitation Spectroscopy.** At low concentrations (<10 $\mu$M), the 77-K emission−excitation spectrum of $[Pt(tpy)Cl]^+$ is nearly superimposable with the room-temperature absorption spectrum. The excitation spectrum of a 5 $\mu$M solution in EMD at 77 K is shown in Figure 8; there are extremely weak features at 463 and 433 nm corresponding to the $^3(\pi \rightarrow \pi^*)$ absorption (associated with the luminescence in dilute solutions). Emission spectra measured with excitation at 436 nm for this dilute solution show the same vibronic progression observed with 366-nm excitation; however, there is a small amount of the broad midrange emission, as well as considerable intensity for the low-energy, metal−metal dimer emission. This is not unexpected, as the $^3(\pi\pi^*)$ molar absorptivity is likely[21] to be only of the order 10 $M^{-1}$ $cm^{-1}$ (*vs* $^1$(MMLCT) absorptivities of 2000−3000 $M^{-1}$ $cm^{-1}$). Very small concentrations of metal−metal dimer may therefore give rise to substantial emission for excitation at this wavelength.

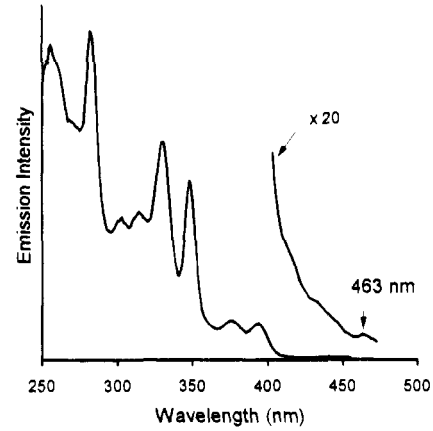


**Figure 8.** Excitation spectra of 5 $\mu$M $[Pt(tpy)Cl]PF_6$ in EMD at 77 K (monitoring emission at 535 nm).

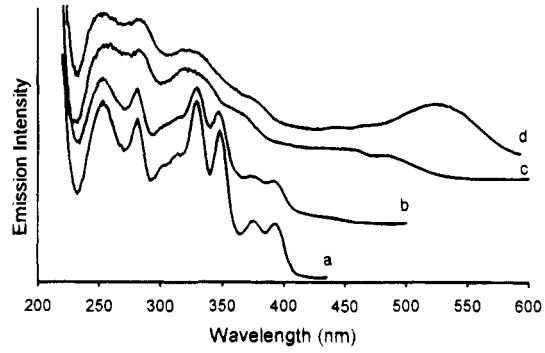


**Figure 9.** Excitation spectra of 0.18 mM $[Pt(tpy)Cl]PF_6$ in EMD at 77 K (monitoring the emission at (a) 475, (b) 580, (c) 680, and (d) 745 nm). The baseline is shifted up for each successive spectrum for clarity. The longest wavelength point in each spectrum corresponds to zero emission intensity.

**Table 5.** Emission Lifetime Data for $[Pt(tpy)Cl]PF_6$ in EMD

| | lifetime, $\tau/\mu$s | | | |
|---|---|---|---|---|
| wavelength/nm[a] | 70 K | 90 K | 110 K | 130 K |
| 740[b] | 1.22 | 1.03 | 0.73 | <0.1 |
| 740 | 1.23 | 1.20 | 1.11 | <0.1 |
| 580 | *c* | 2.45, 15.0[d] | 2.52, 13.4[d] | <0.1 |
| 480 | 13.3 | 12.6 | 13.1 | <0.1 |

[a] Excitation at 355 nm except as noted. [b] Excitation at 532 nm. [c] Data did not fit monophasic or biphasic kinetics well. [d] Biphasic kinetics.

As shown in Figure 9, at higher concentrations the shape of the excitation spectrum is dependent on the observation wavelength. For example, when monitoring between 470 and 550 nm, the spectrum ($[Pt(tpy)Cl]^+$ = 0.15 mM) is almost identical with that measured at low concentration. However, when the emission is monitored between 550−650 nm, the spectrum tails into the 450−550 nm range, and the UV excitation profile broadens substantially. At emission wavelengths >700 nm, the excitation spectrum exhibits a pronounced maximum at ~530 nm.

**Emission Lifetimes.** Lifetimes measured for a 0.15 mM $[Pt(tpy)Cl]PF_6$ solution in EMD at a series of temperatures and emission wavelengths are listed in Table 5. Below the glass transition (~110 K),[25] the lifetimes increase slightly with decreasing temperature.[26] Excitation at 532 nm results in a 740-nm emission band, with a lifetime of ~1 $\mu$s. At higher excitation energies (355 nm), a 580-nm emission band appears with a biphasic decay that was fit to two processes ($\tau_1$ ~ 2.5; $\tau_2$ ~ 14 $\mu$s); the lifetime of the highest energy luminescence (which corresponds to the low-concentration emission spectrum) is about 13 $\mu$s.

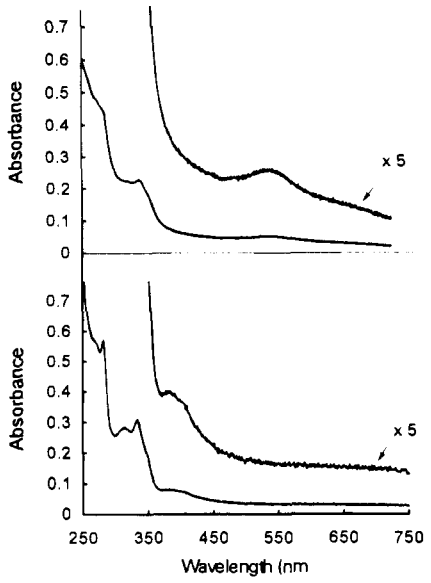


**Figure 10.** Absorption spectra for 0.15 mM [Pt(tpy)Cl]$PF_6$ in EMD: (upper) 77 K; (lower) 298 K.

**Absorption Spectroscopy.** Regardless of the counterion, all $[Pt(tpy)Cl]^+$ salts studied here dissolve to give pale yellow solutions. At low concentration, the absorption spectrum of the $PF_6^-$ salt in DMF shows well-resolved peaks at 272 (36 960), 284 (27 710), 306 (12 630), 318 (12 800), 334 (17 330), 350 (8860), 382 (2760), and 400 nm (2500 $M^{-1}$ $cm^{-1}$), which agree well with the data published for the chloride salt in water.[4] The two lowest energy absorption bands (382, 400 nm) are assigned to an MLCT $^1(d \rightarrow \pi^*)$ transition based on the ligand dependence (red shift) in the series Cl, Br, I.[3c] The next four lowest energy bands (350, 334, 318, 306 nm) are spaced by about 1400 $cm^{-1}$, which fits their assignment as $^1(\pi \rightarrow \pi^*)$. (We note that the tpy $\pi^*$ orbitals are of appropriate symmetry to mix with the $6p_z$ orbital of the Pt center.[27] If this mixing were substantial, the LUMO would best be described as a ($\pi^*$, $p_z$) hybrid. However, for simplicity, we will maintain the $\pi^*$ designation for the LUMO in the following discussion.)

Lippard has shown[4] that the absorption spectra of solutions of the chloride salt do not obey Beer's law in the UV region and has attributed this behavior to oligomerization reactions analogous to those[3b] of $[Pt(CN)_4]^{2-}$; however, no new bands were reported that could be assigned to dimer or oligomer transitions. We have found that when pale yellow DMF solutions of [Pt(tpy)Cl]$PF_6$ are frozen, the solution turns red. The low-temperature (77 K) absorption spectrum of a glassy solution of 0.18 mM $[Pt(tpy)Cl]^+$ in EMD is shown in Figure 10; in addition to a general broadening of bands in the UV region, the spectrum shows a new band at about 510 nm. Although this feature drastically weakens when the solution is warmed through the glass transition temperature, very concentrated aqueous solutions do show a visible absorption band (maximum at about 470 nm) at room temperature (Figure 11). The concentration dependence of this band does not follow Beer's law, and it has a low-concentration $\epsilon$ near zero.

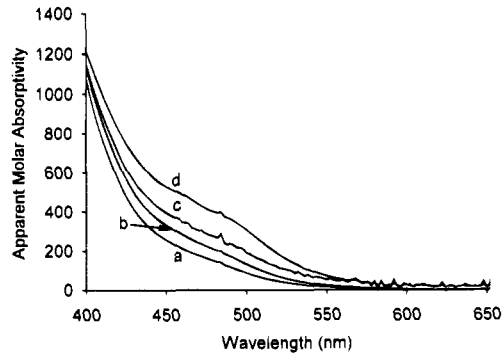


**Figure 11.** Visible absorption spectra of [Pt(tpy)Cl]Cl in aqueous solution plotted as apparent molar absorptivities for (a) 1, (b) 2, (c) 4, and (d) 10 mM.

From studies of the concentration dependence of the UV absorbance, Lippard calculated a dimerization constant for $[Pt(tpy)Cl]^+$ of 4(2) × $10^3$ $M^{-1}$ in 0.1 M NaCl(aq).[4] The apparent molar extinction coefficients in the UV decrease with increasing $[Pt(tpy)Cl]^+$ concentration, apparently because the UV absorption bands of oligomers are broader than those of monomers; indeed, we have observed similar effects for dimerization of the complex in DMF solution.[27] Our UV data, analyzed by the above method,[4] gave a dimerization constant of 3(2) × $10^3$ $M^{-1}$.

When we attempted to fit the 470-nm data assuming that a single dimer was responsible for the concentration dependence, the calculated $\epsilon$ value at 470 nm was only about 1000 $M^{-1}$ $cm^{-1}$.[28] This value is low relative to those of authentic metal–metal bonded Pt–tpy dimers,[2] which all show visible MMLCT absorption bands with molar absorptivities greater than 2000 $M^{-1}$ $cm^{-1}$. A possible explanation is that not all dimers feature metal–metal interactions.

In a minimal model, we assume that there are two dimerization processes, yielding $\pi$–$\pi$ and metal–metal (MM) dimers:

$$2Pt \overset{K_{\pi\pi}}{\rightleftharpoons} (Pt_2)_{\pi\pi} \quad (1)$$

$$2Pt \overset{K_{MM}}{\rightleftharpoons} (Pt_2)_{MM} \quad (2)$$

A general treatment of this case shows that there is an interdependence of $\epsilon$ and the different Ks, and that the dimerization constant determined from the UV data is the sum $K_{\pi\pi} + K_{MM}$:

$$\left(\frac{\epsilon_M - \frac{A}{[Pt]}}{[Pt]}\right)^{1/2} = \left(\frac{2}{\alpha\epsilon_M - \left(\frac{\beta}{2}\right)}\right)^{1/2}\left(\frac{\alpha A}{[Pt]} - \frac{\beta}{2}\right) \quad (3)$$

[Pt] = total Pt concentration

$$\alpha = K_{MM} + K_{\pi\pi}$$

$$\beta = \epsilon_{MM}K_{MM} + \epsilon_{\pi\pi}K_{\pi\pi}$$

If the dimer absorption band in the visible region is due to the metal–metal dimer alone, we have

(25) The glass transition temperature was estimated to be 115–120 K by observation of the loss of cracks in a glassy solution with increasing temperature regulated by a CTI Cryogenic refrigerator.

(26) When the temperature was raised above the glass transition, the only observed signal was one similar to that of the laser pulse shape (pulse width about 20 ns). This is due either to an extremely short lifetime, or to extremely weak emission (in which case the observed signal may be primarily due to laser scatter).

(27) Hill, M. G.; Bailey, J. A.; Miskowski, V. M.; Gray, H. B. Manuscript in preparation.

(28) The equation used,

$$\frac{[Pt]}{\sqrt{A}} = \frac{1}{\sqrt{\epsilon K}} + \frac{2}{\epsilon}\sqrt{A}$$

is analogous to that used by Lippard,[4] and derives from the general case (see text).

$$\frac{[Pt]}{\sqrt{A}} = \frac{1}{\sqrt{\epsilon_{MM}K_{MM}}} + \left(\frac{2}{\epsilon_{MM}} + \frac{2K_{\pi\pi}}{\epsilon_{MM}K_{MM}}\right)(\sqrt{A}) \qquad (4)$$

A plot of $[Pt]/\sqrt{A}$ vs $\sqrt{A}$ should give a straight line with slope of $(2/\epsilon_{MM} + 2K_{\pi\pi}/\epsilon_{MM}K_{MM})$ and $y$ intercept of $1/\sqrt{\epsilon_{MM}K_{MM}}$. This plot is shown in Figure 12. Assuming an $\epsilon_{MM}$ of 2000 $M^{-1}$ $cm^{-1}$ (based on values for Pt–Pt bonded tpy dimers),[2] $K_{MM} = 1.3(1) \times 10^3$ and $K_{\pi\pi} = 1.0(1) \times 10^3$ $M^{-1}$.

## Discussion

There are at least three independent transition types observed in the emission spectra of $[Pt(tpy)Cl]^+$ in glassy solutions. Moreover, the absorption and emission–excitation spectra of this cation are highly dependent on concentration. The limiting low temperature, low-concentration emission spectrum appears very similar to the tpy-localized $^3(\pi \rightarrow \pi^*)$ emission spectra of other metal–tpy compounds,[29] all of which show sharply defined peak progressions (1000–1400 $cm^{-1}$) corresponding to terpyridine vibrational modes. And, again in all cases, relatively long lifetimes are associated with these emissions. We have identified two weak features that correspond to triplet absorptions in the emission–excitation spectrum of a dilute solution of $[Pt(tpy)Cl]^+$, the lower energy of which (463 nm) overlaps nicely with the highest energy line of the dilute solution emission; this feature may therefore be assigned as the $^3(\pi\pi^*)$ 0–0 line. The separation of the second excitation line from the origin (1500 $cm^{-1}$) is similar to the vibronic spacing of the emission, and both of these excitation lines are insensitive to concentration, indicating that they are monomer features.

The longest-wavelength luminescence (740 nm) resembles the MMLCT $^3(\pi^* \rightarrow d\sigma^*)$ emission observed for $\{[Pt(tpy)]_2(\mu\text{-L})\}^{3+}$ complexes.[2] It presumably arises from a dimeric structure in which there is a metal–metal interaction. A moderately intense visible absorption feature (470–510 nm, $\epsilon \geq 1000$ $M^{-1}$ $cm^{-1}$), which was shown to originate from a dimeric species, appears prominently in the excitation spectrum of the long-wavelength emission, and is very similar to the MMLCT $^1(d\sigma^* \rightarrow \pi^*)$ absorption of the bridged binuclear complexes.

The midrange luminescence (550–650 nm) is more difficult to assign. The appearance of similar broad emissions for concentrated solutions of pure terpyridine, or for solutions containing terpyridine and a low concentration of the platinum complex, suggests that the luminescent species does not involve platinum–platinum interactions. There are similarities to the excimer phosphorescence of tethered biarene molecules such as 1,3-di-α-naphthylpropane.[30] For the particular case of $[Pt(tpy)Cl]^+$ dimers, conformations such as that sketched below could account for the $\pi\pi^*$ excimer-like 550–650-nm emissions of the rigid glassy solutions.

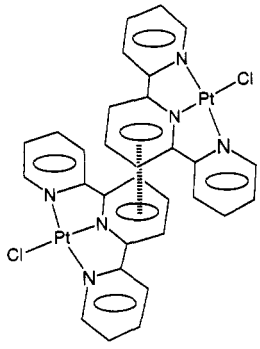


Under these conditions, the excited state of a dimer that is (weakly) bound in a $\pi$-$\pi$ conformation in the ground state cannot rearrange to a metal–metal-bonded conformation. The broad visible luminescence may then be a composite of the emissions from the various non-metal–metal-bound dimeric conformations that are possible. However, it is interesting that these emissions are similar in width and energy to that observed for the *crystalline* compound $\{[Pt(tpy)]_2(\mu\text{-pz})\}(ClO_4)_3 \cdot CH_3CN$,[2] which has a long Pt–Pt distance of 3.432 Å. This compound exhibits only monomer-like $^3(\pi\pi^*)$ emission in frozen polar solvents, while either as a solid or as a frozen (77 K) $CH_3CN$ solution, it displays a broad ($\lambda_{max} = 650$ nm) emission. We proposed[2] a solvent-induced crossover between $^3(\pi\pi^*)$ and $^3$(MMLCT) emissive states. The $^3(\pi\pi^*)$ state in question here may have significant tpy–tpy $\pi\pi$ excimer character near the crossover, and the amount of MMLCT character is debatable for such a long ground-state metal–metal distance. Excimeric $\pi\pi^*$ emission has been invoked to explain the very broad emission of solid $[Pt(bpy)_2]^{2+}$ and $[Pt(phen)_2]^{2+}$ (phen = 1,10-phenanthroline) salts[21a] for which steric effects probably prevent short Pt–Pt distances. The similarly broad room-temperature emissions observed for the solid yellow and orange $[Pt(tpy)Cl]^+$ salts also may have $\pi\pi$ excimer character.[31]

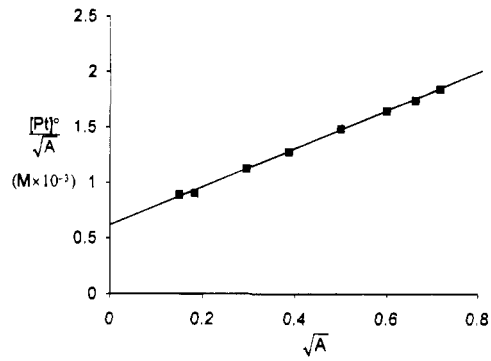


**Figure 12.** Dimerization plot for the concentration range 0.005–2 mM of [Pt(tpy)Cl]Cl in 0.1 M NaCl(aq).

In fluid solution, we observe only the metal–metal (MMLCT) dimer emission, and that only at or below 150 K. Other types of excimers may conceivably convert to the metal–metal-bonded one in fluid solution. The radiative rate constant of the $^3$MMLCT state is likely to be much larger that those of the other emissive states,[16,21] so it should dominate the emission if all excited states are relatively short-lived. That the $^3$MMLCT state itself is short-lived is noteworthy, however. Bridged $\{[Pt(tpy)]_2(\mu\text{-L})\}^{3+}$ complexes display weak ($\phi \approx 10^{-4}$) $^3$MMLCT emission from room-temperature fluid solution,[2] while some Pt(II) α-diimine complexes such as $[Pt(4,4\text{-}(t\text{-}Bu)_2bpy)(CN)_2]$ display moderately intense ($\phi \approx 10^{-3}$) $^3(\pi\pi^*)$ monomer and $\pi\pi^*$ excimer emissions from fluid solution.[32] Because fluid-solution luminescence (attributed to monomer MLCT) from $[Pt(tpy)X]^+$ (X = NCO, OH, $OCH_3$) has been reported,[33]

(29) (a) Ohno, T.; Kato, S.; Kaizaki, S.; Hanazaki, I. *Inorg. Chem.* **1986**, *25*, 3853. (b) Ayala, N. P.; Flynn, C. M., Jr.; Sacksteder, J. N.; Demas, J. N.; Degraff, B. A. *J. Am. Chem. Soc.* **1990**, *112*, 3837.

(30) Lim, E. C. *Acc. Chem. Res.* **1987**, *20*, 8.

(31) We can conceive of several alternative assignments for such a broad emission, which is much too broad for an MMLCT transition.[2] First, $^3$(d-d) emissions of Pt(II) are commonly this broad.[16b] Second, a monomer-like MLCT state of the type $(d_{xz,yz} \rightarrow \pi^*)$ should give broader emission than the MMLCT state because the $d_{xz,yz}$ orbitals are involved in bonding interactions with the tpy ligands, so excited-state distortions from the ground state should be larger. Both of these assignments are unlikely, however, in light of the comparison to the dilute-solution emission.

(32) (a) Che, C.-M.; Wan, K.-T.; He, L.-Y.; Poon, C.-K.; Yam, V. W.-W. *J. Chem. Soc., Chem. Commun.* **1989**, 943. (b) Wan, K. T.; Che, C.-M.; Cho, K.-C. *J. Chem. Soc., Dalton Trans.* **1991**, 1077.

(33) Aldridge, T. K.; Stacey, E. M.; McMillin, D. R. *Inorg Chem.* **1994**, *33*, 722.

we suspect that a thermally accessible $^3$LF excited state[16,21] may be involved in the efficient nonradiative decay of the various excited states of $\{[Pt(tpy)X]^+\}_n$ complexes in fluid solution. That is, any or all of these states (other than $^3$LF) may be intrinsically long-lived in solution, but the weak-field chloride ligand produces a low activation barrier for nonradiative decay of the $\{[Pt(tpy)Cl]^+\}_n$ excited states.

**Acknowledgment.** We thank C.-M. Che, N. S. Lewis, and G. R. Rossman for experimental assistance and helpful discussions. This work was supported by the National Science Foundation and the Office of Naval Research.

**Supporting Information Available:** Figures S-1 (packing diagram for the unit cell of $[Pt(tpy)Cl]ClO_4$) and S-2 (reflectance spectra of $[Pt(tpy)Cl]X$, $X = ClO_4^-$ (red and orange forms), $Cl^-$, $PF_6^-$, $CF_3SO_3^-$); and Tables S-I–S-IV (crystallographic data, assigned hydrogen atom parameters, anisotropic displacement parameters, and complete distances and angles for $[Pt(tpy)Cl]ClO_4$) (9 pages). Ordering information is given on any current masthead page.

IC940777R